Proceedings of the 5th International Symposium on Steel Science (ISSS 2017)
Nov. 13-16, 2017, Kyoto, Japan: The Iron and Steel Institute of Japan

Phosphorus-assisted delamination toughening in high-strength steel

Yuuji Kimura[1*], Xiaohua Min[2], Takashi Kimura[1], Kaneaki Tsuzaki[3]

[1] National Institute for Materials Science, 1-2-1 Sengen, Tsukuba, Ibaraki, 305-0047, Japan
[2] Dalian University of Technology, Dalian 116024, P.R. China
[3] Kyushu University, 744 Motooka, Nishi-Ku, Fukuoka, 819-0395, Japan

Abstract: Fe-0.4%C-1%Cr-0.7%Mn-0.2%Mo alloy (in mass%) was selected as a base material. 100 kg ingots with different Phosphorus (P) contents from 0.001% to 0.093% were prepared by vacuum melting and hot-rolled after homogenizing at 1200 ºC for 1 h. Ultrafine elongated grain (UFEG) structures with a strong <110>//rolling direction fiber texture were created through deformation of tempered martensitic structures by multi-pass calibre-rolling with a cumulative rolling reduction of 78% at 500 ºC (warm tempforming) and then annealed at 550 ºC for 1 h. There was little influence of the P addition on the UFEG structure and the strength of the tempformed samples. The average values of room temperature yield and tensile strength of tempformed samples were 1060 and 1130 MPa, respectively. However, delamination perpendicular to the notch orientation of the impact specimens was observed to occur during V-notch Charpy impact testing, and the delamination was pronounced as the P content increased. As a result of delamination, the tempformed sample with an addition of 0.093% P exhibited an inverse temperature dependence of toughness at temperatures from -20 to 80 ºC, in which intergranular fracture along the prior-austenite grain boundaries occurred in the martensitic samples that were tempered at 550 ºC for 1 h. The delamination toughening was demonstrated to be dominated by the UFEG structure, and further assisted by the P segregation. Furthermore, P was heterogeneously distributed in segregation bands, which provided a structure consisting of brittle and ductile layers, and this was considered to be especially effective in promoting the delamination toughening.

1. INTRODUCTION

Phosphorus (P) is usually considered as an undesirable impurity in high-strength steels because P segregation at grain boundaries enhances the intergranular embrittlement [1]. For example, in JIS alloy steel for machine structural use such as JIS SCM 440, P content is limited to be 0.03 mass% or less. Meanwhile, a part from its embrittlement effect, the P addition is known to improve hardenability and atmospheric corrosion resistance of steels. Hence, if we can use P as an alloying element, it is a great advantage in practical application of high-strength steels.

The two most important control parameters for the notch toughness of structural materials are their intrinsic fracture resistance and the operative stress system under which the fracture occurs [2]. For example, the grain refinement is an effective method not only for strengthening of structural materials but also for improving the intrinsic fracture resistance. As the grain size is decreased, the stress concentration and the segregated impurity concentration are reduced at the grain boundaries, leading to the suppression of the intergranular fracture [3]. On the other hand, delamination toughening is well-known in pipe line steels [4], laminate composites [5] with anisotropic microstructures, etc. Delamination can relax the triaxial tension stresses generated by the localized plastic constrain at the notch and/or the crack tip ahead of advancing crack tips, enhancing notch toughness.

Kimura et al. [6-11] have developed delamination toughening in ultra-high-strength steels with ultrafine elongated grain (UFEG) structures that were processed by multi-pass caliber rolling of tempered martensitic structures at an elevated temperature (i.e., warm tempforming). They found out an inverse temperature dependence of toughness at sub-zero temperatures, as a consequence of delamination that occurred perpendicular to the notch orientation of the impact specimens [6-11]. Furthermore, Jafari et al. [12-15] investigated delamination toughening in a

* Corresponding author. E-mail: KIMURA.Yuuji@nims.go.jp, telephone: +81 29 859 2123.

0.4%C-1%Cr-0.7%Mn-0.2%Mo steel with an addition of 0.053% P and observed that the P addition enhanced the delamination toughening for warm tempformed sample at temperature from -150 to 150 ºC, at which intergranular fracture occurred for the conventionally quenched and tempered sample. The delamination is considered to be promoted through the reduction of the interface cohesion due to the P segregation in the UFEG structure [12-15].

In this paper, we will report the influence of P addition on the microstructure, tensile properties, and V-notch Charpy impact properties for 0.4%C-1%Cr-0.7%Mn-0.2%Mo steels with different P contents ranging from 0.001% to 0.093% [16]. Warm tempforming by multi-pass caliber rolling at 500 ºC with a cumulative rolling reduction of 78% was applied to the steels to create the UFEG structures. A special attention was paid to the influence of P segregation bands on the delamination toughening.

2. EXPERIMENTAL

2.1. Materials preparation

Table 1 shows the chemical compositions of the P steels. Fe-0.4%C-1%Cr-0.7%Mn-0.2%Mo alloy (in mass%) was selected as a base material. The chemical compositions of these steels are similar to that of the JIS SCM 440 (AISI 4140) steel, with the exception of the high P content. 100 kg ingots with a thickness of about 20 cm were prepared by vacuum melting, and hot-rolled into plates with a thickness of 4 cm after homogenizing at 1200 ºC for 1 h. The blocks of 12 cm (l) ×4 cm (w) × 4 cm (t) were cut from the hot-rolled plates, homogenized at 1200 ºC for 0.5 h, and caliber-rolled into square bars with a cross-section of 9 cm^2, followed by air cooling. The rolled bars were austenitized at 920 ºC for 0.5 h, followed by oil quenching. The quenched bars were tempered at 500 ºC for 1 h, and tempformed by multi-pass caliber rolling with a cumulative rolling reduction of 78% into square bars with a cross-section of 2 cm^2, followed by air cooling. The tempformed bars were annealed at 550 ºC for 1 h, followed by water cooling (TF samples). For a comparison, some of TF samples were normalized at 880 ºC and austenitized at 920 ºC for 0.5 h, followed by oil quenching. The quenched bars were tempered at 550 ºC for 1 h, followed by water cooling (QT samples).

Table 1. Chemical compositions of the P steels (mass%).

Steels	C	Si	Mn	Cr	Mo	P	S
0.001%P	0.40	0.24	0.73	1.04	0.22	0.001	<0.001
0.018%P	0.40	0.24	0.70	0.99	0.20	0.018	<0.0005
0.053%P	0.42	0.25	0.72	0.98	0.20	0.053	0.001
0.068%P	0.40	0.25	0.71	1.01	0.20	0.068	<0.0005
0.093%P	0.41	0.24	0.71	1.00	0.20	0.093	0.0005

2.2. Microstructural observation and mechanical testing

The microstructures were observed by optical microscopy and field emission scanning electron microscopy (FE-SEM). The EBSD analysis was performed using a FE-SEM (JEOL JSM-6500F) equipped with an orientation imaging microscope. The step size was 0.05 μm in an area of 25 μm × 25 μm. The elemental distributions of the samples were mapped by FE-EPMA (JXA-8500F) with a specific resolution of 2 μm.

Tensile tests were performed for round bar specimens with a parallel length of 42 mm and a diameter of 6 mm at a crosshead speed of 0.85 mm/min. Charpy impact tests were carried out for full-size 2 mm V-notch specimens over the temperature range of -196 to 350 ºC.

3. RESULTS

3.1. Microstructures

Fig. 1 shows the microstructures in the QT and TF samples with an addition of 0.093% P. The QT sample exhibits typical tempered martensitic structure. The equiaxed prior-austenite grains with an average grain size of approximately 30 μm are subdivided by the packet and block boundaries (Fig. 1(a, d)). In the grain boundary map, the grain boundaries with a misorientation angle of 10° or over mainly reflect the block boundaries (Fig. 1(d)). The average linear intercept length for the block structure was thus measured to be 0.60 μm. Besides, cementite particles are spherical and film-like grain boundary cementite particles, which facilitate the intergranular fracture, are not observed (Fig. 1(f)). On the other hand, through the warm tempforming, the blocks, packets, and prior-austenite

grains were elongated in the rolling direction (RD) and their boundaries were destroyed (Fig. 1(b)). As a result, UFEG structure with a strong <110>//RD fiber texture was evolved for the TF sample (Fig. 1(c, e)). In the UFEG structure, the average linear intercept length of the grain boundaries with a misorientation angle of 10° or over was measured to be 0.4 μm in the transverse direction, and 1.2 μm in the longitudinal direction. When compared to the QT sample, the cementite particles for the TF sample are more spherical (Fig. 1(g)). The long axes of cementite particles are almost aligned to the RD. The transverse grain size, grain shape, <110>//RD fiber texture, and cementite particle distribution for the TF sample with an addition of 0.093% P were confirmed to be almost comparable to those of the TF samples with P contents of 0.001% and 0.053% [12-15]. Hence, in P content up to levels of 0.093%, the P addition had little influence on the evolution of the UFEG structure during the warm tempforming. Similarly, the influence of P addition on the tempered martensitic structure was observed to be negligibly small in the QT samples [12-15].

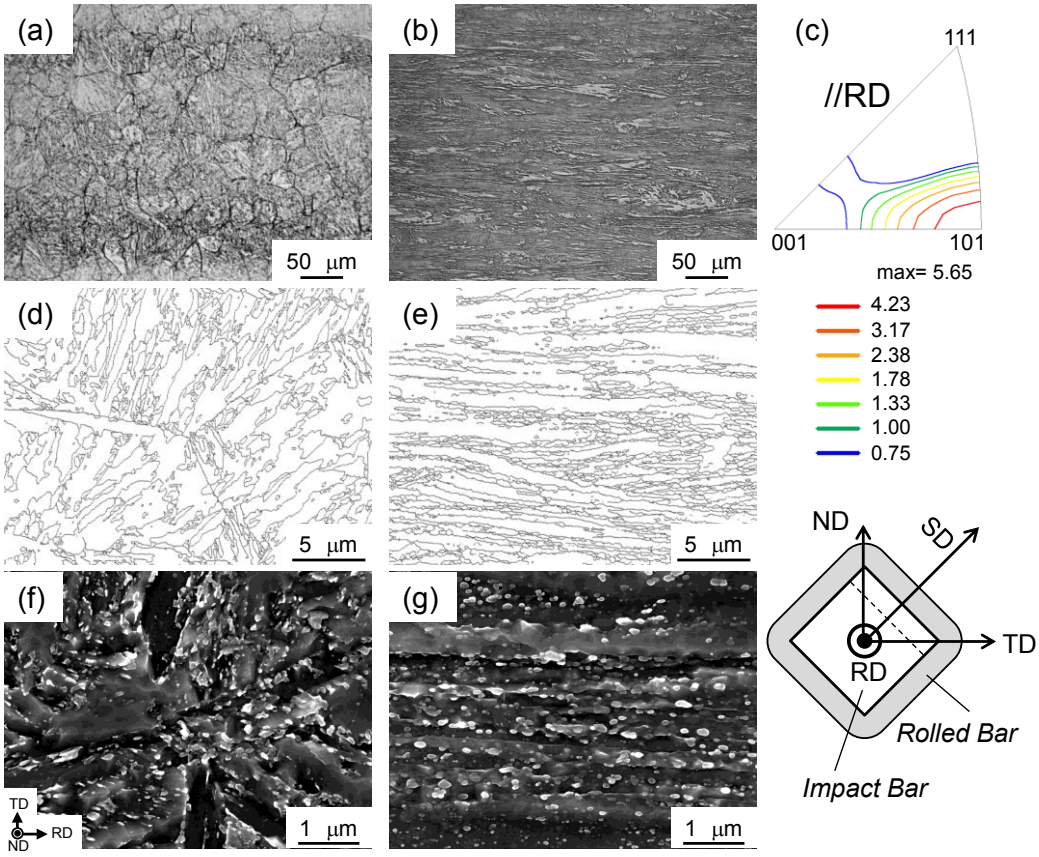

Fig. 1. Microstructures of the QT (a, d, f) and TF (b, e, g) samples. Inverse pole figure for the rolling direction (RD) (c) shows the development of a strong <110>//RD fiber texture for the TF sample. Boundaries with a misorientation angle of 10º or over are indicated by dark lines in (d, e). The schematic drawing indicates the relation between RD and the sample position. The ND and TD are normal to RD. The striking direction (SD) of the impact bar has an angle of 45º to the TD and ND.

3.2. Tensile properties

Fig. 2 shows the nominal stress and strain curves in the QT and TF samples with an addition of 0.093% P. It was characteristic that all the QT samples exhibited a continuous yielding, while all the TF samples exhibited an obvious yield drop during discontinuous yielding. Such a yield drop phenomena was often observed in ultrafine grained materials, and it was usually accompanied by plastic instability [17-18]. However, the TF samples exhibited a yield drop followed by adequate uniform elongation. Tensile properties of the QT and TF samples are summarized in Fig. 3, as a function of P content. There are no significant differences in the yield and tensile strength of the TF samples. Similar trend was observed in the QT samples. Hence, the P addition up to levels of 0.093% was demonstrated to have little influence on the strength for the QT and TF samples. The respective

average values of the yield and tensile strength for the TF samples are 1060 and 1130 MPa. The tensile strength of the TF samples is almost comparable to that of the QT samples, while the yield strength of the TF samples tends to be slightly higher than that of the QT samples, in connection with a difference in the yielding behavior. Furthermore, the P addition has little influence on the uniform elongation of the TF samples (7–8%), as well as that of the QT samples (5–6%). On the other hand, the P addition tends to decrease the post-uniform elongation and reduction in area in both QT and TF samples; however its influence is larger in the QT sample than in the TF sample.

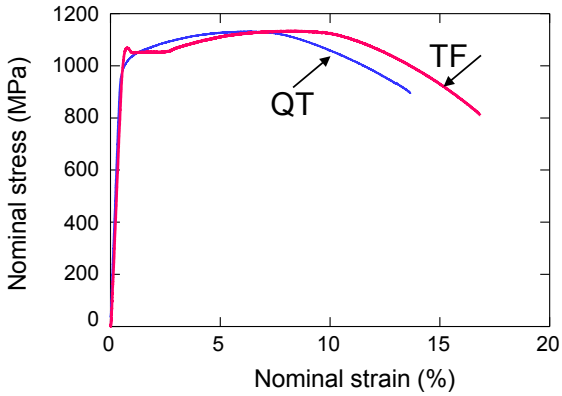

Fig. 2. Nominal stress and strain curves for the QT and TF samples with an addition of 0.093% P.

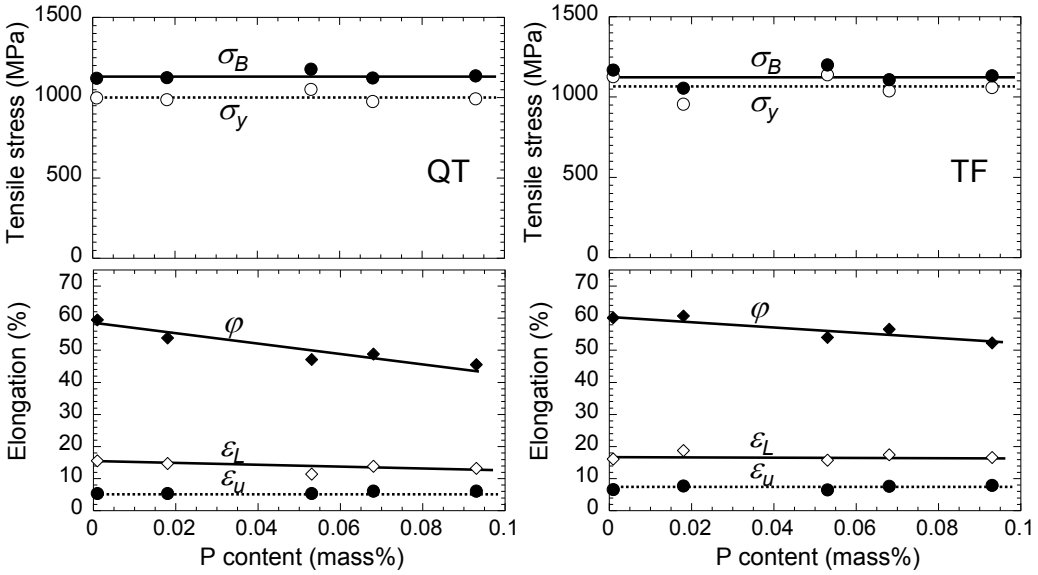

Fig. 3. Yield strength (σ_y), tensile strength (σ_B), uniform elongation (ε_u), total elongation (ε_L), and reduction in are (φ) for the QT and TF samples as a function of P content.

3.3. V-notch Charpy impact properties

Fig. 4 (a) shows the variations in the absorbed energy at room temperature for the QT and TF samples as a function of P content. The absorbed energy for the QT sample markedly decreases with the addition of P; it decreases from 93 to 7 J on average as the P content increases from 0.001 to 0.093%. By contrast, the absorbed energy for the TF samples maintains an almost constant average value of 140-150 J in the P content up to levels of 0.05%, above which it markedly increases. The 0.093% P addition enhanced the absorbed energy up to196 J on average. Fig.4 (b) displays the fracture appearances of impact bars. For all the QT samples, the crack propagated across the central portion of the impact bar. In the P content of 0.018% or less, shear lips developed at the edges of the specimens. A similar ductile failure was also observed in the TF sample with the P content of 0.018% or less. However, for the TF samples containing 0.068% and 0.093% P, delamination was observed to occur in the longitudinal direction of impact bars and it was especially pronounced in the TF sample with an addition of 0.093% P. Hence, the delamination toughening was observed for the TF samples.

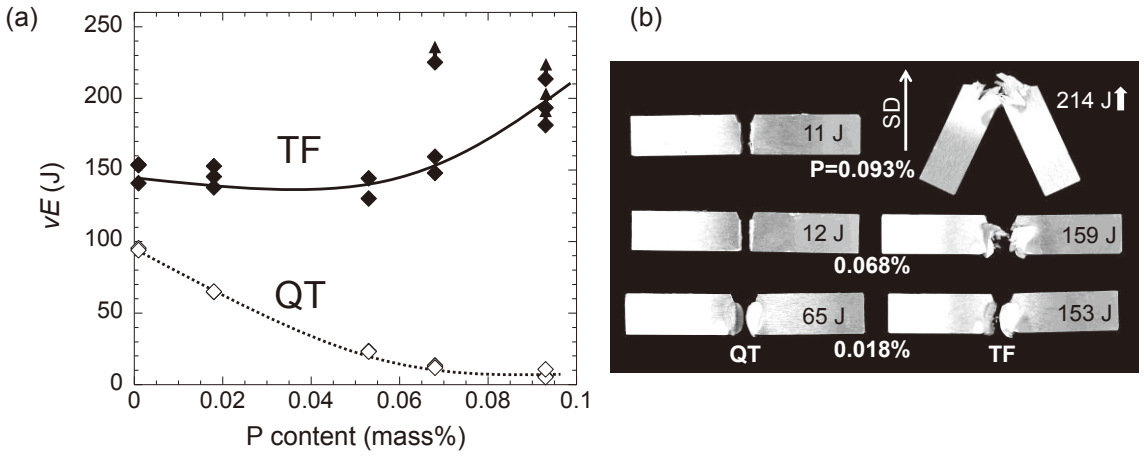

Fig. 4. Change in V-notch Chapry absorbed energy (*vE*) as a function of P content (a) and fracture appearances of the specimens after impact testing (b). Arrows in (a, b) indicate the specimens, which did not separate into two pieces during impact testing.

Fig. 5 shows the change in the absorbed energy as a function of testing temperature for the TF and QT samples containing 0.001% and 0.093% P. Since, none of the TF samples exhibited delamination at 350 ºC, the absorbed energy at 350 ºC was defined as upper-shelf energy. Although the 0.093 % P addition for the TF samples tends to reduce the upper-shelf energy from 149 to 134 J, the upper-shelf energy for the TF sample is higher than that of the QT sample without the P addition (98 J). The upper-shelf energy for the QT sample is reduced to 57 J by the addition of 0.093% P. Such trends are similar to those in the post-uniform elongation and reduction in area in Fig. 3. Furthermore, delamination fracture regions are indicated by dash arrows. The TF samples exhibit the delamination toughening at lower temperature, at which the absorbed energy for the QT samples is reduced as a result of brittle failure. Here, it should be noted that the delamination toughening was confined to a narrow temperature range in the vicinity of -150 ºC for the TF sample without the P addition, while it occurred over a wide temperature range from -150 to 250 ºC for the TF sample with an addition of 0.093% P. The TF sample with an addition of 0.093% P also exhibited a significant inverse temperature dependence of toughness at the temperature range of from -20 to 80 ºC. As a result, the TF sample with an addition of 0.093% P has superior impact properties, compared to the QT sample without the P addition. Therefore, the addition of P was demonstrated to be effective to control the delamination toughening of the high-strength steels with an UFEG structure, especially in the P content range of 0.05 % to 0.09%.

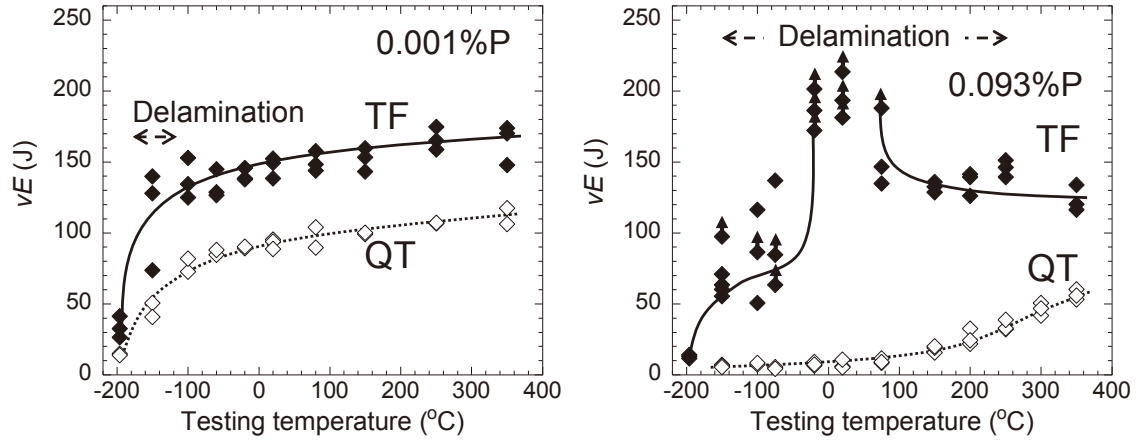

Fig. 5. Change in V-notch Chapry absorbed energy (*vE*) as a function of testing temperature. Arrows indicate the specimens, which did not separate into two pieces during impact testing. An inverse temperature dependence of toughness is observed at temperature from -20 to 80 ºC for the TF sample with an addition of 0.093% P.

4. DISCUSSION

When the delamination occurs in the geometry of the crack-arrester as shown in Fig.6 (a), the notch is blunted and the triaxial tension stress condition in the process zone at the notch tip of the specimen is relaxed towards a state of uniaxial tension; the impact specimen virtually behaves as an un-notched specimen. Also, the stress fielding effect from the formation of microcracks along the longitudinal direction of the notched specimens can reduce the driving force for fracture [19]. As a result, a high absorbed is obtainable.

Delamination fracture occurs when the tensile stress along the SD of the notched specimen exceeds the critical brittle fracture stress along the SD. If we assume the Tresca yield criterion in the process zone within the plastically yielding region of the notch root, the maximum values of the tensile stress along the RD and SD in the process zone can be approximated on the basis of yield strength (σ_y) as 2.6 × σ_y and 1.6 × σ_y [20], respectively. Therefore, there are two methods to control delamination toughening; one is to increase the σ_y of the steels and the other is to reduce the brittle fracture stress along the SD.

For the UFEG structure with a strong <110>//RD fiber texture, many {100} cleavage planes are distributed on the planes along the RD and on the transverse planes with the angle of ±45º to the RD as shown in Fig.6 (c). The {100} coherence length is longer in the RD than in the transverse directions with an angle of 45º. This microstructure also has good grain boundary continuity along the RD owing to the elongated grain shape. Hence, the brittle cracks easily propagate on these weakest interfaces and/or planes along the RD (Fig.6 (b)). On the other hand, {100} cleavage planes scarcely exist on the planes normal to the RD (Fig.6 (c)); the cleavage crack barely propagates in the SD. This gives a condition for the occurrence of delamination in the UFEG structure. Since the TF sample without the P addition exhibits delamination at -150 ºC (Fig.5), it may be concluded that the UFEG structure with a strong <110>//RD fiber texture is a key factor for delamination to occur. The P addition can further assist the occurrence of delamination through reducing the brittle fracture stress along the SD. Jafari et al. indicated that P might segregate to the weak interfaces, such as the grain boundaries, ferrite matrix/cementite interfaces, and {100} planes, and consequently decreased the interface cohesion [13]. However, the ductility and toughness in the planes normal to the RD were not significantly degraded by the addition of P. This may lead to the delamination toughening at higher temperatures.

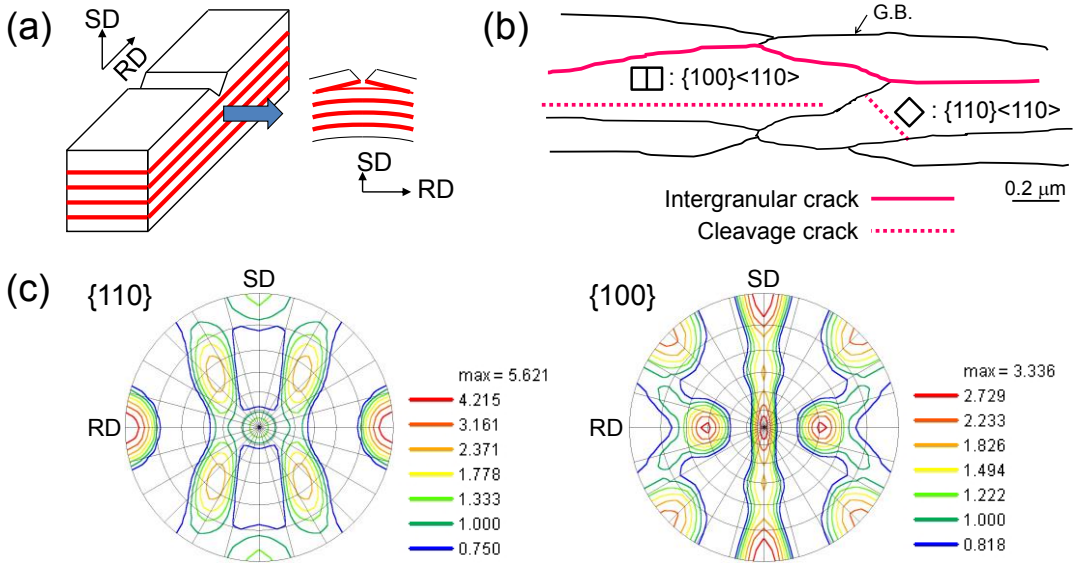

Fig. 6. Schematic illustrations showing the delamination in crack-arrester geometry (a) and brittle crack propagation in the ultrafine elongated grain (UFEG) structure with a strong <110>//RD fiber texture (b). {110} and {100} pole figures for the UFEG structure are also shown.

Additionally, let us consider the influence of P segregation bands inherited from the solidification process of the ingot. Fig. 7 is an example of the P concentration line profiles for the TF samples as a function of the P content. The P segregation bands became more distinct as the P content increased, especially in the 0.093% P content. For example, the P concentration in the high P concentration regions appears to reach up to about 0.15 mass%, while it is close to 0.05 mass% in the low P concentration region.

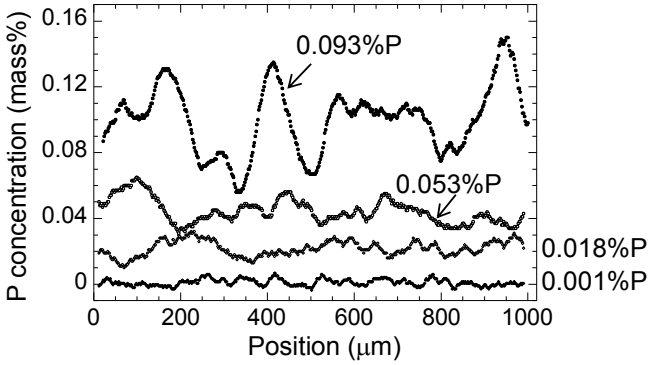

Fig. 7. P concentration line profiles for the TF sample as a function of P content.

Fig. 8 shows the relation between the crack propagation and P segregation band for the QT and TF samples with an addition of 0.093% P that were subjected to Charpy impact testing at -20 ºC. At the same cumulative rolling reduction, no significant difference in the P segregation bands was observed between the QT and TF samples. In the both samples, the segregation bands with high (red color) and low (blue and green color) P concentrations are co-existent along the RD. For the QT sample, the cracks propagated along the prior-austenite grain boundaries without being influenced by the P segregation bands. This was because the prior-austenite grain structure was isotropic and P concentration might be much higher at the boundaries of prior-austenite grains than the segregation bands. Auger electron spectroscopy analysis on the intergranular facet indicated that P concentration at prior-austenite grain boundaries was approximately 2 mass% on average for the QT sample with an addition of 0.053% P [21]. On the other hand, for the TF sample, delamination cracks were observed to preferentially propagate along the P segregation bands with high P concentration regions, as shown in Fig. 8(d, e). This might be especially effective to promote delamination toughening compared to the homogeneous distribution of P. In the high P concentration regions, the brittle cracks can initiate and propagate along the RD without any significant deflection at higher temperatures. On the other hand, in the low P concentration regions, the UFEG structure may maintain high ductility and toughness at lower temperatures. Therefore, the highly ductile UFEG structure combined with the brittle P segregated bands might lead to enhanced delamination toughening over a wide temperature range of -150 to 250 ºC for the TF with an addition of 0.093%P.

Our strategy to enhance the toughness of high-strength steel is to arrest the propagation of the main cracks along the transverse directions in the hierarchical, anisotropic, and ultrafine grain structure [6-11, 19-20]. These findings further indicate that the use of the solidification structure is effective to enhance the toughness of high-strength steel with an UFEG structure.

5. SUMMARY

The addition of P, up to 0.093% (mass%), had little influence on the evolution of the ultrafine elongated grain (UFEG) structure and the strength of 0.4%C-1%Cr-0.7%Mn-0.2%Mo steels that were processed by warm tempforming using multi-pass calibre rolling at 500 ºC with cumulative rolling reduction of 78%. On the other hand, the P addition enhanced delamination toughening for the warm tempformed steels with an UFEG structure. The delamination toughening was dominated by the UFEG structure, and further assisted by the phosphorus segregation. The formation of distinct P segregation bands, which presented a structure consisting of brittle and ductile layers, might be especially effective in accelerating delamination and improving toughness in the warm tempformed steel in a wide temperature range. Therefore, it was demonstrated that P might be used as an alloying element in the high-strength steel with a hierarchical, anisotropic, and ultrafine grain structure.

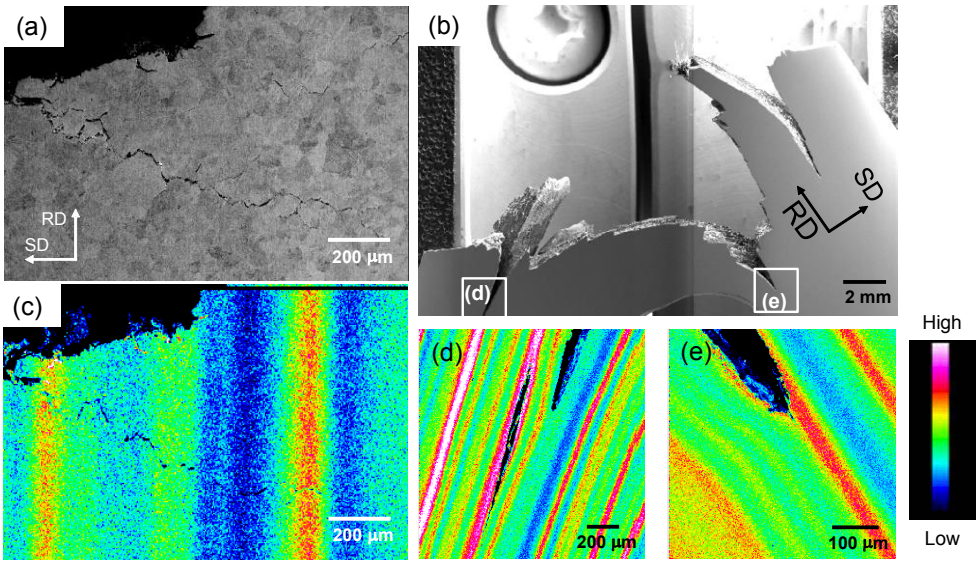

Fig. 8. SEM images (a, b) and FE-EMPA mappings (c-e) showing the relations between crack propagation and P segregation bands in the QT (a, c) and TF (b, d, e) samples. Charpy impact test was performed at -20 ºC.

Acknowledgements: We thank Mr. Kuroda and Mr. Taniuchi for the caliber-rolling processing of the materials, and Ms. Hirota and Mr. Nishio for their assistance with the SEM and EPMA observations. This study was partly supported by CREST, Japan Science and Technology Agency.

REFERENCES

[1] H. Ohtani, C. J. McMahon Jr.: Acta Metall. 23 (1975), 377–386.
[2] J. D. Embury, N. J. Petch, A. E. Wraith, E. S. Wright: Trans. Metall. Soc. AIME, 239(1967), 114–118.
[3] R.P.M. Proctor, H.W. Paxton, Trans. ASM 62 (1969), 989–999.
[4] B. Mintz, W. B. Morrison: Mater. Sci. Technol., 23(2007), 1346–1356.
[5] D. W. Kum, T. Oyama, J. Wadsworth, O. D. Sherby: J. Mech. Phys., 31(1983), 173–186.
[6] Y. Kimura, T. Inoue, F. Yin, K. Tsuzaki: Science, 320 (2008), 1057–1060.
[7] Y. Kimura, T. Inoue, F. Yin, K. Tsuzaki: ISIJ Int., 50 (2010), 152–161.
[8] Y. Kimura, T. Inoue: Metall. Mater. Trans. A, 44A (2013), 560–576.
[9] Y. Kimura, T. Inoue: ISIJ Int., 55 (2015), 1135–1144.
[10] Y. Kimura, T. Inoue: ISIJ Int., 55 (2015), 1762–1771.
[11] Y. Kimura, T. Inoue: ISIJ Int., 56 (2016), 2047–2056.
[12] M. Jafari, Y. Kimura, Y. Nie, K. Tsuzaki: ISIJ Int., 50 (2010), 1660–1665.
[13] M. Jafari, Y. Kimura, K. Tsuzaki: Metall. Mater. Trans. A 43 (2012) 2453–2465.
[14] M. Jafari, Y. Kimura, K. Tsuzaki: Adv. Mater. Res. 409 (2012) 231–236.
[15] M. Jafari, Y. Kimura, K. Tsuzaki: Phil.Mag. Lett. 93 (2013) 109–115.
[16] X. Min, Y. Kimura, T. Kimura, K. Tsuzaki: Mater. Sci. Eng. A, 649 (2016), 135–145.
[17] S. Takaki, K. Kawasaki, Y. Kimura: J. Mater. Process. Technol., 117(2001), 359–363.
[18] N. Tsuji, N. Kamikawa, R. Ueji, N. Takata, H. Koyama, D. Terada: ISIJ Int., 48(2008), 1114-1121.
[19] T. Inoue, Y. Kimura, S. Ochiai: Scripta Mater., 65(2011), 552–555.
[20] T. Inoue, Y. Kimura: J. Mater. Sci., 48(2013), 4766–4772.
[21] M. Jafari, K. Tsuzaki: J. Alloys and Compounds, 577S(2013), S636-S641.